Synthesis of Mesoporous MgO Nanostructures for Enhanced Adsorption And Antimicrobial Application

A

Dissertation submitted

In the partial fulfilment of the requirement for the degree of

M.Sc. (Chemistry)

Submitted by

Jyoti Sharma

(301402008)

Under the supervision of:

Dr. Soumen Basu

Assistant Professor

School of Chemistry & Biochemistry

Thapar University, Patiala-147004

July 2016

CERTIFICATE

This is to certify that Ms. JYOTI SHARMA has completed the M.Sc. Chemistry in School of Chemistry and Biochemistry dissertation entitled "**SYNTHESIS OF MESOPOROUS MgO NANOSTRUCTURES FOR ENHANCED ADSORPTION AND ANTIMICROBIAL APPLICATION**" under my guidance and supervision. To the best of my knowledge, the present work is the result of her original investigation and study. No part of the dissertation has ever been submitted for any other degree or diploma at any university. The dissertation is fits for the submission and the fulfilment of the conditions for the award of M.Sc. chemistry.

Date: 30th June, 2016

Dr. Soumen Basu (Supervisor)
Assistant Professor
SCBC, Thapar University, Patiala

Dr. Bonamali Pal
Head of SCBC
Thapar University, Patiala

Dr. S.S. Bhatia
Dean, Academic Affairs,
Thapar University, Patiala-147004

DECLARATION

I hereby declare that the material presented in this dissertation entitled "**SYNTHESIS OF MESOPOROUS MgO NANOSTRUCTURES FOR ENHANCED ADSORPTION AND ANTIMICROBIAL APPLICATION**" in the partial fulfilment for requirements of the award of the degree in Masters of Science in Chemistry and being submitted to the department of Chemistry and Biochemistry, Thapar University, Patiala, is my own work during the period of January to July 2016, under the supervision of **Dr. Soumen Basu.** I have not submitted the contents embodied in this dissertation for the award of any other degree.

Date: 15th July 2016

Jyoti Sharma
301402008
M.Sc. Chemistry

This is to certify that the statement made by the candidate is correct and true to the best of our knowledge.

Dr. Soumen Basu
Assistant Professor
SCBC, Thapar University

Dr. Bonamali Pal
Head, SCBC

ACKNOWLEDGEMENT

First and foremost, I would like to express my sincere and deepest appreciation to my M.Sc. dissertation thesis supervisor, **Dr. Soumen Basu**, Assistant Professor, School of Chemistry & Biochemistry, Thapar University, Patiala - 147004, India for his valuable discussions and suggestions, guidance, strong motivation, encouragement and inspiration throughout my M.Sc. dissertation thesis journey.

I also express my heartiest gratitude to **Dr. Bonamali Pal**, Head and Professor School of Chemistry & Biochemistry, Thapar University, Patiala - 147004, India for his constant support throughout the period.

I would like to express my deepest gratitude to my beloved Family, **Mr. Durga Dutt Sharma, Mrs. Meena Dutt Sharma** and **Mr.Vishal Sharma** who have always believe in me, and endured with me during difficult times

I invariably fall short of words to express my heart-felt gratitude and profound thanks to my seniors **Miss Manisha Sharma, Miss Akansha Mehta and Mr. Amit Mishra** for their valuable suggestions and inspiring discussions. I wish to express my thanks to them for their cooperation and help during the course of my research work.

Deepest thanks to the friends who have always been with me; **Miss Yashika Raparia, Miss Devyani Thapliyal, Miss Sheenam Kaushal, Miss Mandeep Kaur** from M.Sc. and all other friends from M.Sc. and research scholars of School of Chemistry & Biochemistry, Thapar University.

Date: 15. July, 2016

Sharma

Jyoti Sharma

ABSTRACT

MgO was synthesised via surfactant-templating method. Different ratios of mixture of surfactants were used to increase the surface area. Highest surface area was recorded with C_{16}TAB:SDS was 179.81 m^2g^{-1}. Synthesised sample were characterised by FTIR, SEM, XRD, TEM, and BET. The adsorption study and antimicrobial activities was done. The maximum adsorption capacities were (333.33, 250 and 200) mg g^{-1} for methylene blue, alizarin and rhodamine, respectively. MgO also has a very good use as a bactericide. The antimicrobial activity of MgO was also checked on *E.coli* and *B.Subtilis* and their IC_{50} values obtained after 24h were 0.476±0.056 and 0.449±0.043, respectively.

Table of Contents

CHAPTER 1- INTRODUCTION

Nanotechnology is design, fabrication and application of nanostructures or nanomaterials, and the fundamental understanding of the relationships between physical properties or phenomena and material dimensions. Nanotechnology deals with materials or structures in nanometer scales, typically ranging from micronanometers to several hundred nanometers on nanometer scale, materials or structures may possess new physical properties or exhibit new physical phenomena. One nanometer is 10^{-3} micrometer or 10^{-9}meter. Nanoparticles have unique properties which differs it from the bulk materials. There are many nanoparticles such as CaO, ZnO, TiO_2, SiO_2, MgO. MgO is a homomorphous compound and has a rock salt structure. It has stable configuration with comparatively small number of electrons. It has well defined surface defect structures such as low coordinated ions/or vacancies. MgO is an attractive material which has many potential applications[1], such as water purification, optoelectronics, microelectronics, and additive in heavy fuel oil, paint, gas separation, bactericides, and insulator in industrial cables, crucibles, and refractory materials[2-15].

In the latest years, MgO is preferred for the catalytic research and surface structure analysis[16-18]. Nanocrystalline MgO exhibits adsorbent properties due to both better surface areas and intrinsically higher surface reactivities. MgO is the main inorganic material exhibits a wide band-gap[19]. In medicinal area, MgO is used for the relief of sore stomach, bone regeneration and heartburn[20].

1.1 Electronic Structure

The electronic properties of nanostructures of metals and insulators have been widely used investigated as they originate transport and optical phenomena in these materials.

Bulk materials posses a partially filled electronic band and their ability to conduct electrons are due to the availability of a continuum of energy levels above the fermi energy, E_f. MgO has wide gap between conduction band and valence band which comes into the category of insulator. The electronic band between valence band and conduction band is 5ev.

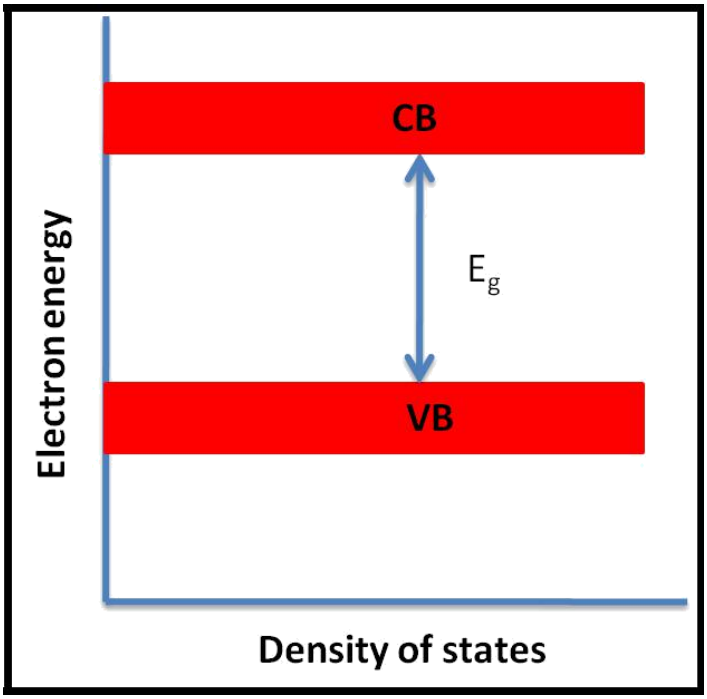

Figure 1.1: Wide band gap of MgO between conduction band and valence band

1.2 USES of MgO

Potential uses of magnesium oxide nanoparticles are:

MgO is act as a High-temperature dehydrating agent which is used in the production of silicon steel sheet.

It is also high-grade ceramic material, adhesive and additive in the chemical raw material and electronic industry material.

Due to its insulating nature it is used for making crucible, electrode bar, insulated conduct electrode, and sheet smelter.

In radio industry, high-frequency magnetic-rod antenna, insulating material filler, magnetic device filler and various carriers used in radio industry.

In chemical fibre and plastics trades MgO used as a fire.

In refractory fibre and refractory material, magnesite-chrome brick, filler for refractory coating, refractory and insulating instrument, electricity, cable, optical material, material for steel-smelting furnace and other high-temperature furnaces, heating material and ceramic base plate

Fuel additive, cleaner, antistatic agent and corrosion inhibitor.

Mesoporous materials have been of great interest for the researchers, as it exhibits many applications i.e., useful in many industries, in food borne diseases, dye adsorption, metal doping. Mesoporous MgO with high specific surface areas acts as a disparaging adsorbent for toxic chemical agents. MgO has distinguished structure that exhibit many properties such as optical electronic, magnetic, mechanical, thermal, and chemical properties[21-24].

1.3 MgO as a Bactericide

Nanoparticles considered as antibacterial agents due to its surface properties, size and structure[25]. There are inorganic and organic antibacterial agents which are involved in bacterial control[26], but mainly the Inorganic antibacterial agents have improved stability even in insensitive conditions[27].Inorganic antibacterial agents such as TiO_2, ZnO, MgO and CaO have also discussed[28].Out of these MgO is stable as well as considered as safe materials for human beings[29].MgO is not only used in bacterial control but is also used as a antimicrobial agents without using photoactivation[30]

1.4 MgO as adsorbent

Metal oxides have potential applications in water treatment due to their high surface area added to low production and regeneration costs. The rapid industrialization over the past few decades imposes a major threat on environment due to synthetic dyes in industrial effluents. Approximately 10–15% of the dyes are wasted into environment worldwide after their use in the dyeing units. Since the dyes are stable, recalcitrant, colorant and even potentially carcinogenic and toxic, their release into the environment poses serious environmental, aesthetical and health threats so their removal from the industrial effluents is a major environmental issue. Among physical, chemical and biological conventional methods of dye removal, physical adsorption is an effective method for fast removal of dyes from the effluents. Many adsorbents such as activated carbon[31], silica[32], clay[33], natural and synthetic polymers[34], waste materials[35-36] and various nanotubes[37-38] are available. Even then it would be desirable if more effective and cheaper adsorbent with higher adsorption capacity and recycling ability is developed.

Adsorption is considered to be safest and less expensive remedy to handle this problem than precipitation, ion exchange and membrane filtration. An ideal absorbent

is one with uniformly accessible pores, an interlinked pore system, have high surface area, physical and chemical stability.

During the past few years, mesoporous materials have gained a lot of interest as adsorbents for heavy dyes and harmful organic compounds, owing to their ultrahigh surface area, tuneable pore size and volume. They also allow molecular accessibility to large internal volumes and surface areas. Mesoporous adsorbents have good adsorption capacity and been proved to have great advantages than traditional adsorbents like activated charcoal and resins.

CHAPTER 2-LITERATURE REVIEW

There are two important aspects of nanotechnology i.e, synthesis and processing of nanomaterials and nanostructures. Organic materials play a crucial role, like surfactants plays an important role in the synthesis of ordered mesoporous materials and capping polymers in the synthesis of monodispersed nanoparticles.

MgO is synthesised by many methods such as:

1. Microwave assisted synthesis ,
2. Wet chemical method,
3. Nonaqueous sol gel method,
4. Surfactant assisted precipitation method ,
5. Combustion,
6. Hard templating pathway,
7. Spinning disk reactor,
8. Wet chemical method or chemical synthesis,
9. Electrospinning technique,
10. Colloidal synthesis,
11. Rf impulse discharge plasma
12. Microwave hydrothermal process

These are the methods which have been used for the synthesis of nanoparticles MgO. Including this ,there are many precursors such as glycine, $Mg(CHCOO)_2$, polyvinyl alcohol, $MgCl_2$, $MgCl_2.6H_2O$, magnesium nitrate, magnesium acetate tetrahydrate, various fuels, urea, combination of urea, 1,3 propane diol, have been used.

Magnesium oxide is mainly obtained by the thermal decomposition of magnesium carbonates or hydroxide. Magnesium hydroxide is used as the precursor in the synthesis of magnesium oxide. Magnesium hydroxide is frequently used as the flame-retardant filler in composite materials as it undergo endothermic dehydration in fire conditions or from nitrate and from precursor of acetate solution and in recent times by sol gel process.

A sol-gel method is a promising technique for the formation of magnesium oxalate dihydrate followed by annealing at a suitable temperature to form MgO. The advantages are its simplicity, cost-effectiveness, low reaction temperature, high surface area-to-volume ratio, narrow particle size distribution and high purity of the

final product. Early attempts to prepare magnesium oxalate dihydrate were by using either magnesium methoxide or magnesium ethoxide that was reacted with oxalic acid in ethanol to form a precursor based on the sol-gel reaction.

Jimmy C.Yu and co workers in 2004, analysed that porous $Mg(OH)_2$ was prepared by simple hydrothermal method from bulk MgO. These thin plates would accumulate in the large globular particles. The plate like morphology was obtained and posses a wormhole-like porous structure with high surface area. After calcination, porous MgO nanoplates were obtained. Aggregation of nanoplates leads to large mesopores of size about 36nm and every plate has small wormhole mesopores of size about 3.7 nm.

Meng-Fu Zhu and co workers in 2013, reported that by catalytic degradation, oil pollutants can be removed from water in which nano-MgO can used as catalyst. The study determined that nano-MgO on the oil pollutant was associated with the dosage of nano-MgO by catalytic degradation. When oil content was 1.8 mg/L, 0.17 g nano-MgO was used and the removal rate of oil was 93.92%.

Li-Zhai Pei and co-workers in 2010, proposed synthesis of magnesium oxide and magnesium aluminate ($MgAl_2O_4$) spinel (MAS) powders synthesized by sol-gel process using citrate polymeric precursors derived from magnesium chloride, aluminium nitrate and citrate. Single phase cubic MgO powder and MAS powder form after heat treatment at 800˚C and 1200°C was obtained.

Xin-Yao Yu and co workers in 2011, reported a facile method was also used to obtain porous micro-/nanostructured MgO. Nest-like or Flower-like MgO was obtained through adjusting the concentration of precipitant. It also used as a adsorbent for the removal of As (III) and As(V).

Cuiling Gao and co-workers in 2008, reported that MgO can also synthesised by adjusting the composition and phase structure of magnesium carbonate hydrate (MCH). The phase structure of the MCH is varied from monoclinic $Mg5(CO_3)4(OH)_2(H_2O)_4$ to hexagonal $MgCO_3$ by adjusting the concentration of Mg^{2+}

and HCO_3^- msesoporous MgO exhibits excellent adsorption capacity for heavy metal ions and a adsorbent in waste water treatment.

Juncheng Hu and co workers in 2010, reported that nanoplates of MgO with polar (111) facet as the primary surface can be considered as adsorbents for dye pollutants removal from wastewater. The thickness of the MgO (111) nanoplates is (3 to 5) nm, with an average particular surface area of 198 $m^2 g^{-1}$. Congo red and reactive brilliant red X3B are used as dyes, and their adsorption is observed at different dye concentrations, temperatures, salt concentration, and solution pH and in a batch process. The maximum adsorption capability of congo red on MgO (111) nanosheets were approached to 131.3 mg g^{-1} in 30 min. The Langmuir and Freundlich isotherms, were used to explain the interaction of dye and MgO (111). The maximum adsorption capacities were (303.0 and 277.8) mg g^{-1} for Congo red and reactive brilliant red X3B, respectively. They had also considered the adsorption kinetic data followed a pseudo-second-order rate for both dyes. Adsorbent MgO (111) nanoplates can be regenerated by the calcination process and reused.

Table 2.1: Literature review of the surfactant used for synthesis of mesoporous MgO

Author/year	specifications	Surfactant	Surface area	adsorption	References
Zi-sheng chao and co-workers (2002)	Surfactant templating method.	CTAB, SDS, SDBS, MTAB, DTAB.	CTAB+SDS = 219.72 m^2g^{-1}	No study	44
Hong Yan and co workers (2008)	Hydrothermal method	CTAB	Surface area Was not calculated.	No study	39
Mehran Rezaei and co workers (2010)	Simple precipitation method.	PEG	160.9m^2g^{-1}	No study	22
Juncheng Hu and co-workers (2010)	Green method in the absence of urea.	No surfactants were used.	198 m^2g^{-1}	303.0 and 277.8) $mg \cdot g^{-1}$ for congo red and briliiant red.	39
Jimmy C.Yu and co workers (2003)	hydrothermal method	No surfactants were used.	Mesopore size 3.7nm	No study	42

Objectives

- To Synthesise Porous MgO with high surface area.
- To study the effect of surfactants (CTAB+SDS) on the porous structure of MgO.
- Adsorption of toxic dyes by MgO.
- To study the antimicrobial activity of MgO.

CHAPTER 3- MATERIALS AND METHODS

3.1 Materials

3.1.1 Magnesium chloride: Magnesium chloride is the chemical compound with the formula $MgCl_2$ and its various hydrates $MgCl_2(H_2O)_x$. Their salts are ionic halides and highly soluble in water. Hydrates of $MgCl_2$ can be obtained from sea water or brine. It acts as a precursor in many magnesium compounds. For example by precipitation method.

$MgCl_{2(aq)} + NaOH_{(aq)} \rightarrow Mg(OH)_{2(s)} + NaCl_{(S)}$

3.1.2 Cetyltrimethyl ammonium bromide (CTAB):

CTAB is a cationic surfactant. It is useful in antiseptic agent against bacteria and fungi. The cetrimonium chloride and cetrimonium stearate are used as topical antiseptics. CTAB forms micelles in aqueous solutions. Its micellar aggregation number is 75-120 at 303K.

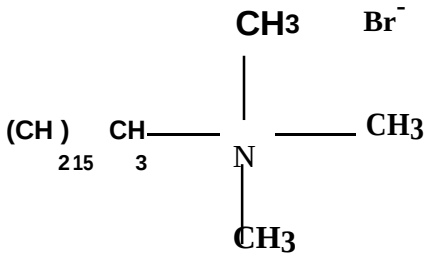

Figure 3.1: Structure of CTAB

3.1.3. Sodium dodecyl sulfate (SDS):

Sodium dodecyl sulfate (SDS) is an anionic surfactant, synonymously sodium lauryl sulfate is a synthetic pharmaceutical, and food products, as well as of industrial and commercial cleaning and product formulations. It also used in denaturation of proteins.

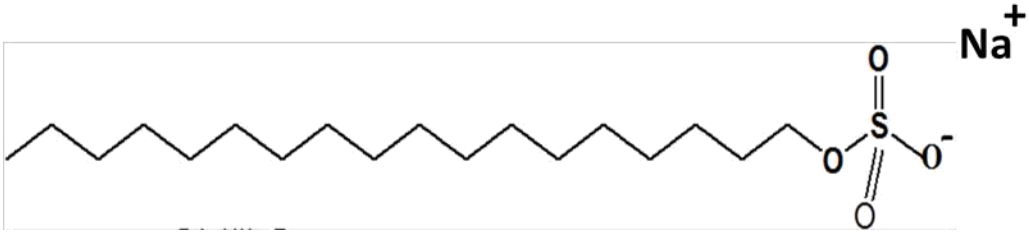

Figure 3.2: Structure of sodium dodecyl sulfate

3.2 Dyes

3.2.1 Methylene blue:

Methylene blue also known as **methylthioninium chloride**. Methylene blue is used as a medication and dye. It is a heterocyclic compound with the chemical formula $C_{16}H_{18}N_3SCl$. At room temperature it appears as a solid, dark green powder, odourless, that yields a blue solution when dissolved in water.

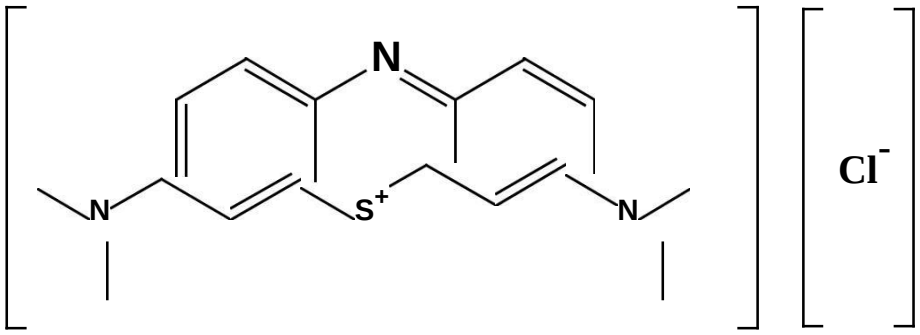

Figure 3.3: Structure of methylene blue

3.2.2 Rhodamine:

Rhodamine is a family of related chemical compounds, fluorine dyes. Examples of rhodamine are **Rhodamine 6G and Rhodamine B**. They are used as a dye and as a dye laser gain medium. They are often used as a tracer dye within water to determine the rate and direction of flow and transport. Rhodamine dyes are more popularly in biotechnology applications such as fluorescence microscopy, correlation spectroscopy and ELISA.

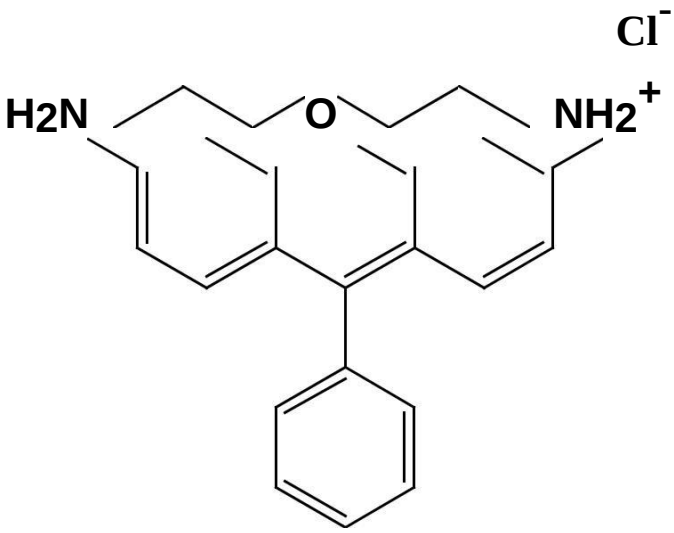

Figure 3.4: Structure of Rhodamine dye

3.2.3 Alizarin:

Alizarin or 1, 2-dihydroxyanthraquinone is also known as Mordant Red 11and Turkey red is an organic compound which has molecular formula $C_{14}H_8O_4$ that has been used as a prominent red dye for dyeing textile fabrics. Historically it was found that this dye was derived from the roots of plants of the madder genus. Alizarin is the main ingredient for the manufacture of Rose madder and Alizarin crimson. It is soluble in chloroform and hexane and has melting point of 277-278˚C. It is used in biochemical essay to determine, quantitatively by colorimeter and the presence of calcify deposition by cells of oestrogenic lineage.

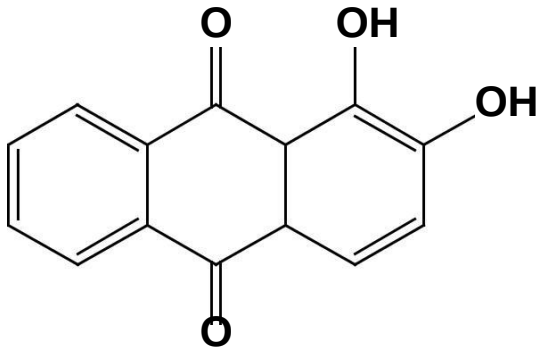

Figure 3.5: Structure of Alizarin dye

3.3 Apparatus

Beakers (50ml and 250 ml), test tubes(10ml), micro pipette, measuring cylinder, forceps, filter paper, glass rod, magnetic beads, Petri plates, flasks(50 ml), crucible, pestle and mortar.

3.4 Instrument Used

3.4.1 Magnetic Stirrer:

A magnetic stirrer of REMI 2MLH is a laboratory device which uses magnetic field to mix liquid samples, since only a small magnetic bar has to put inside the liquid sample to start the process of mixing. It is used in the experiment for the preparation of $Mg(OH)_2$ by mixing $MgCl_2$, CTAB, SDS and NaOH. Magnetic stirrer often includes a hot plate or some other means for heating the liquid.

3.4.2 Weighing Balance:

Accurate quantities of used chemicals can be achieved with the help of weighing balance.

Maximum-250 gm; Denisty-0.01 mg

3.4.3 Hot Air Oven:

The hot air oven also known as digital temp indicator cum controller of PHYSILAB was used to dry the precipitates after the filtration process. Generally they are operated at temperature of 500˚C- 3000˚C using a thermostat to control the temperature.

3.4.5. Laboratory Centrifuge:

Centrifugation is a process that involves use of centrifugal force for the sedimentation of heterogeneous mixtures. This process is used to separate two immiscible liquids. The laboratory centrifuge (PHYSILAB) works under the principle where the centripetal acceleration will cause denser substances to move outward in the radial direction, the substances which are less dense are displaced and move to the centre.

3.4.5 Muffle Furnace:

A muffle furnace (PREFIT INDIA) is box type oven for high temperature applications. These are used in various research labs by chemists in order to determine

the proportion of sample which is non-combustible and non-volatile. It is used to calcine the samples. Calcination is a thermal treatment process for the removal of volatile fraction. Muffle furnace consists of externally heated chamber, so that material being heated has no contact with the flame. This muffle furnace can achieve a maximum temperature of 400˚C.

3.5 Methodology

3.5.1 Preparation of $Mg(OH)_2$:

Step 1: Prepare 1M $MgCl_2$ in 10 ml of solution and 0.5M CTAB and 0.5M SDS in 5ml each. Then prepare freshly sodium hydroxide of 2M solution.

Step 2: After preparation of all the solutions, mix $MgCl_2$, CTAB, SDS on a magnetic stirrer for 1 hour. Then freshly prepared NaOH was added or 30 min of constant stirring.

Step 3: Then dry it in the microwave oven at 80˚C for 24hours.

Step 4: Calcine it at 400˚C/min for 4-5 hours.

By keeping the concentration of $MgCl_2$ constant, and changing the concentration of mixture of surfactants i.e, 1:1 , 1:0.25 , 1:0.5 , 1:2 , 1:3. 1:0.2, the whole above process was repeated.

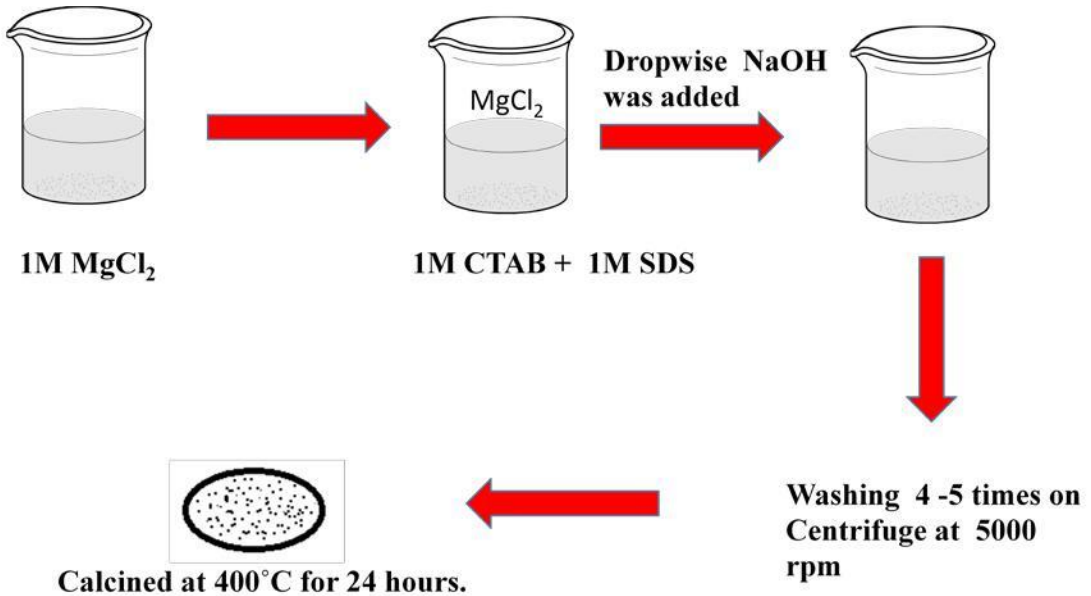

Figure 3.6: Flow chart diagram of synthesis of mesoporous MgO using surfactants.

3.5.2 Preparation of Dye solution

The dye solution was prepared by (1ppm) amount of dye into proper amount of deionised water in a volumetric flask. In, this experiment 0.1mm solution of dye was prepared

Molarity of Mb = 3.19mM

Molarity of Alz = 2.49mM

Molarity of Rod = 4.79mM

3.5.3 Dye adsorption

Dye adsorption was carried out using in dark conditions and the change in concentration prior to adsorption on the mesoporous MgO was monitored UV-Vis spectrophotometer. 1mg of mesoporous MgO was added into 10 ml of aqueous dye solution with different concentration stirring at 200 rpm in dark environment.

3.5.4 Preparation of microbial cultures: Antibacterial activity of MgO was done with the inoculation of *B. subtilis* and *E.coli* bacteria in the aqueous solution of media. After 24h of incubation OD was calculated to check the antibacterial activity.

CHAPTER 4 - CHARACTERIZATION TECHNIQUES

The sample was characterised by XRD PAN ANALYTICAL X'PERT PRO operated at 45KV diffractometer and Cu Kα wavelength of 1.54˚ A in the range of 2θ= 20˚-70˚. The nitrogen adsorption-desorption isotherms were determined at 77 K using a BEL JAPAN gas sorption and porosimetry apparatus and FTIR by Agilent resolution pro carry 660 by KBr pellet method.

4.1 X-Ray Diffractometer

The German physicist M.von Laue (1879-1960) in 1913 suggested the possibility of diffraction of X-rays by crystals. By X-Ray diffraction we can obtain structural information about crystalline solids. It is also helpful in determination of three dimensional structures of many complex biomolecules. It also fills the gaps between physics, chemistry and biology.

Bragg's law is a simplistic model to understand what conditions are required for diffraction.

$$\lambda = 2d_{hkl} \sin\theta \qquad (1)$$

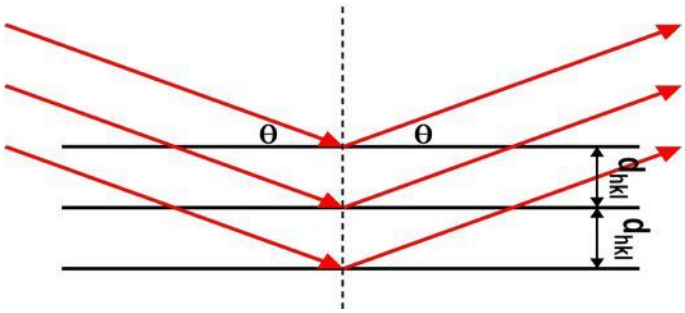

Figure 4.1: Diffraction pattern of XRD

Bragg's law is only satisfied for parallel planes of atoms, with a space d_{hkl} between the planes, constructive interference. X-ray wavelength is fixed in diffractometers. At particular angle q, different families of planes produces a diffraction peaks. In addition to this plane normal should be parallel to the diffraction vector. The space between diffracting planes of atoms determines peak positions.

4.2 Fourier-transform infrared spectroscopy (FTIR)

FTIR spectroscopy is a vibrational spectroscopic technique. It takes advantage of asymmetric molecular stretching, vibration and rotation of chemical bonds as they are exposed to designated wavelengths of light.

4.3 Scanning Electron Microscope (SEM)

A **SEM** is a type of electron microscope that produces images of a sample by scanning it with a focused beam of electrons. The electrons interact with atoms in the sample, producing various signals that contain information about the sample's surface topography and composition. The electron beam is generally scanned in a raster scan pattern and the beam's position is combined with the detected signal to produce an image. SEM can achieve resolution better than 1 nanometer. Specimens can be observed in high vacuum, in low vacuum, in wet conditions (in environmental SEM) and at a wide range of cryogenic or elevated temperatures.

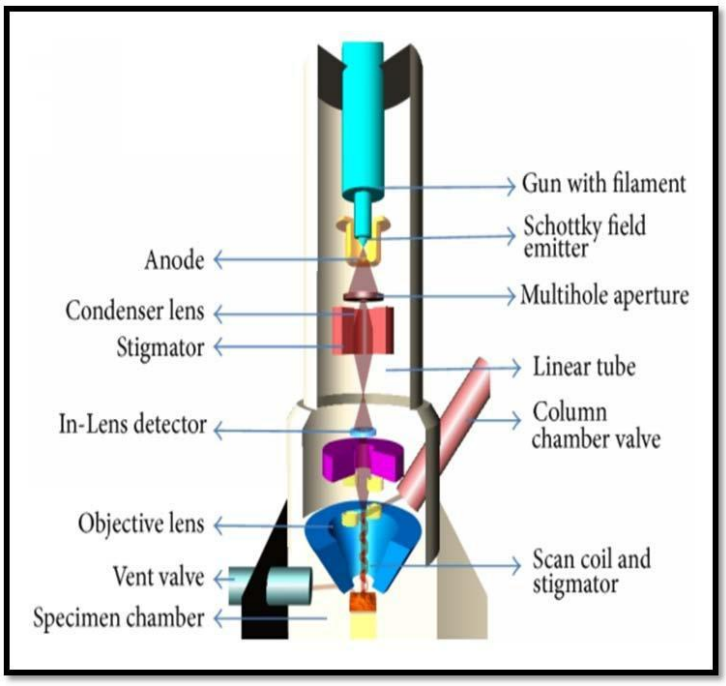

Figure 4.2: Working principle of SEM (Yessi Jusman et al. 2014, Scientific world journal)

4.4 Transmission Electron Microscopy (TEM)

A **TEM** is a microscopy technique in which a beam of electrons is transmitted through an ultra-thin specimen, interacting with the specimen as it passes through it. An image is formed from the interaction of the electrons transmitted through the specimen; the image is magnified and focused onto an imaging device, such as a fluorescent screen, on a layer of photographic film, or to be detected by a sensor such as a CCD camera.

Principal:

Illumination - Source is a beam of high velocity electrons accelerated under vacuum, focused by condenser lens (electromagnetic bending of electron beam) onto specimen.

Image formation - Loss and scattering of electrons by individual parts of the specimen. Emergent electron beam is focused by objective lens. Final image forms on a fluorescent screen for viewing.

4.5 Bruaneur-Emmett-Teller (BET):

The specific surface area of a mesoporous MgO has been determined by physical adsorption of gas on surface of solid and by calculating the amount of adsorbate gas which corresponds to a monomolecular layer on the surface. Physical adsorption results from relatively weak Vander Waals forces between the adsorbate gas molecules and adsorbent surface area of test powder.

In physical adsorption, adsorption isotherms can be classified as one of 6 types, as shown in the Table 4.1.

The theory of adsorption proposed in 1938 by brunaue, Emmett and teller known as BET theory, assumes that physical adsorption resulting in the formation of multilayers, is the true picture of adsorption.

BET equation:

$$q = \frac{q_m K_b C}{[C_a - C]\{1 + [K_b - 1][C / C_a]\}} \qquad (2)$$

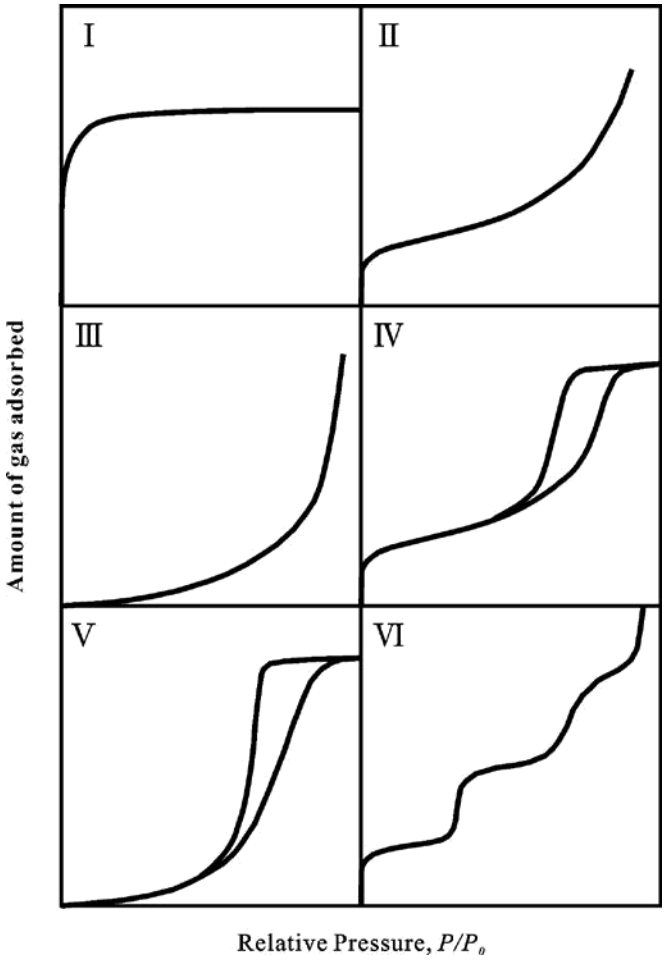

Figure 4.3: Types of adsorption isotherm

Table 4.1: Feature of adsorption isotherm

Type	Interaction between sample surface and adsorbate	Porosity	Sample- adsorptive example
I	Relatively strong	Micropores	Activated carbon-nitrogen
II	Relatively strong	Nonporous	Oxide-nitrogen
III	Weak	Nonporous	Carbon-water vapour
IV	Relatively strong	Mesopore	Silica-nitrogen
V	Weak	Mesopore	Activated carbon-water vapor
VI	Relatively strong	Nonporous	Graphite - krypton

Table 4.2: Sizes of pores classified as

	Pore diameter/nm
Micropore	Upto to 2
Mesopore	2-50
Macropore	50 or up.

CHAPTER 5 - RESULTS AND DISCUSSIONS

Based upon the composition of various samples of mesoporous MgO samples were characterized with the help of different techniques and the respective results were discussed as follows**.**

5.1 XRD:

The meso-structured MgO was synthesized at room temperature of molar composition of $MgCl_2$: CTAB+ SDS. The sample was characterised by XRD PAN ANALYTICAL X'PERT PRO operated at 45KV diffractometer and Cu Kα wavelength of 1.54 ˚Ain the range of 2θ= 20˚-70˚ Figure 1 presents the X-ray diffraction patterns of the samples synthesized with various MgCl2 : CTAB/SDS composition. Figure 1 shows the XRD patterns of the mesoporous MgO which was calcined at 400˚C at 1˚C/min for 5 -6 hours. According to the JCPDS card (JCPDS card, No. 45-0946, the intense peaks show that the powder is highly crystalline. The crystal size of the nanorods range from 30-45nm.

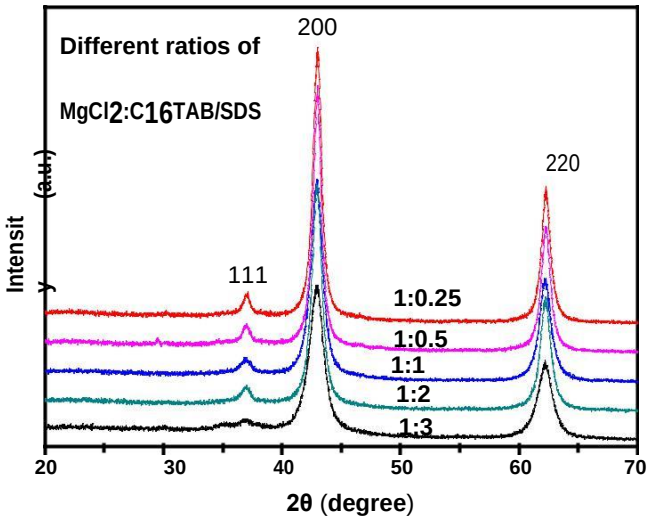

Figure 5.1: X-Ray diffraction pattern of mesoporous MgO.

5.2 FTIR:

Structural characterization of the mesoporous MgO nanoparticles membranes was investigated by FTIR. In the spectra of MgO powder, the broad absorption band at 557.532 cm^{-1} associated with the symmetric Mg=O bond can be observed. The

absorption bands at 3386 cm^{-1} (stretching) and 1439 cm^{-1} (bending) indicate the presence of hydroxyl groups (OH), which is due to the presence of $Mg(OH)_2$ .The bands at 1101.643 cm^{-1} (stretching) is due to the cationic surfactant used.

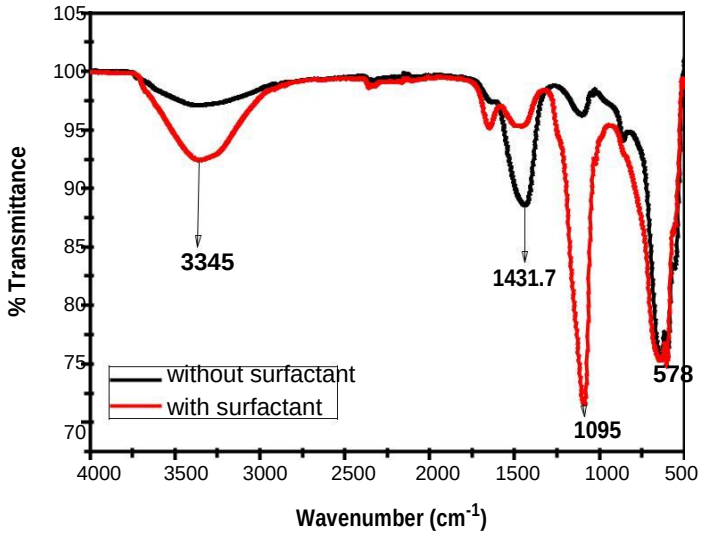

Figure 5.2: FTIR of MgO with and without surfacatnts

5.3 Morphology:

The morphology of MgO was characterised by FESEM and HRTEM analysis. FESEM shows the gives the nanorods of MgO. It gives all the discrete structure such as the spherical and rodlike structure.

5.3.1 SEM:

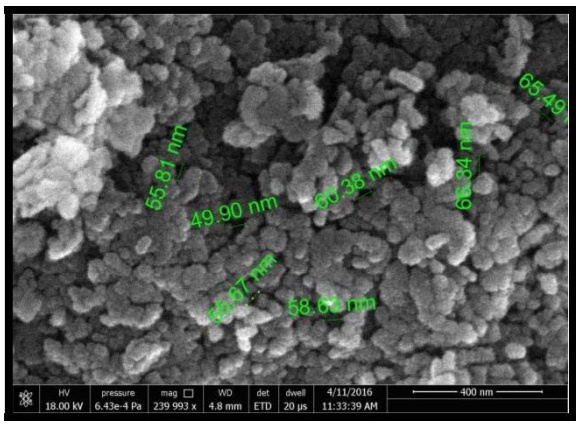

Figure 5.3: SEM images of mesoporous MgO

The morphology and size of the powders are analyzed by SEM observation. Figure 5.3 shows the average diameter of the MgO powders with rod shaped is about 60 nm. However, some particles are in microns size.

5.3.2 TEM:

By, TEM we can calculate the diameter of the nanorods of the mesoporous MgO. The average size of Mgo nanorods calculated through TEM were20-60nm (Figure 5.4) and the same can be correlated with SEM. The particle size bar graph from TEM has been shown in Figure 5.5.

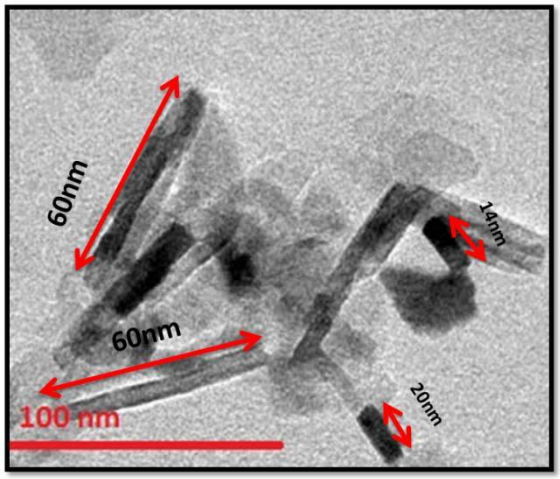

Figure 5.4: TEM image of mesoporous MgO with different nanorods

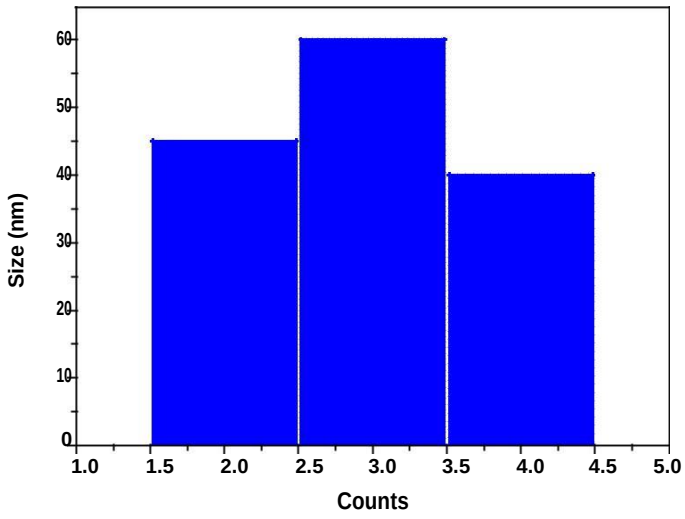

Figure 5.5: Particle size distribution of MgO nanorods through TEM

5.4 Effect of Surfactant:

Surfactant plays a key role to make the compound mesoporous**.** The mixture of anionic and cationic surfactant forms a micellar structure with the precursor. The chain length is an important factor to increase the pore size of the compound.

Table 5.1: Nitrogen adsorption-desorption parameters showing effect of mixture of anionic and cationic surfactants at different ratio on mesoporous MgO.

Sample Name	**Ratio**	**Surface Area (m^2g^{-1})**	**Pore Volume (cm^3g^{-1})**	**Pore Size (nm)**
$MgCl_2$:C_{16TAB}+SDS	1:0.25	164.65	0.7863	19.103
$MgCl_2$:C_{16TAB}+SDS	1:0.5	141.25	1.2821	36.305
$MgCl_2$:C_{16TAB}+SDS	1:1	137.52	1.1898	34.608
$MgCl_2$:C_{16TAB}+SDS	1:2	60.63	0.7039	46.437
$MgCl_2$:C_{16TAB}+SDS	1:3	136.52	1.4968	43.855

Table 5.2: Nitrogen adsorption-desorption parameters showing effect of chain length of cationic surfactant using mixture of cat-anionic surfactants for mesoporous MgO.

Sample Name	**Ratio**	**Surface Area (m^2g^{-1})**	**Pore Volume (cm^3g^{-1})**	**Pore Size (nm)**
C_{18}tab : SDS	1:0.25	49.8	0.7391	59.331
C_{16}tab:SDS	1:0.25	109.42	0.9782	35.761
C_{14}tab : SDS	1:0.25	147.13	1.3382	36.381
C_{12}tab :SDS	1:0.25	171.89	1.4867	34.596

In all cases, nanorods of MgO with an interconnected mesoporous structures were obtained. The N_2 sorption isotherms (Microtrac Belsorp, Bel, Japan, Inc.) of mesoporous MgO synthesized with different ratio of CTAB and SDS are shown in Figure 5.4. It is clearly seen that the relative pressure (P/P_0) at which a fixed increase in the adsorption was observed which was shifted to higher values with increasing molar ratios. The BET areas increased from 60m^2/g to 171.49 m^2/g, with increase in the chain length of CTAB and with decrease in ratio. The uniformity of pore sizes and shape were defined by the sharp adsorption and desorption branches in H1 hysteresis loops of the synthesized mesoporous MgO. On the other hand, pore volume of the MgO significantly varied due to the variation of mesopore size (0.7 – 1.7 cm^3 g^{-1}).

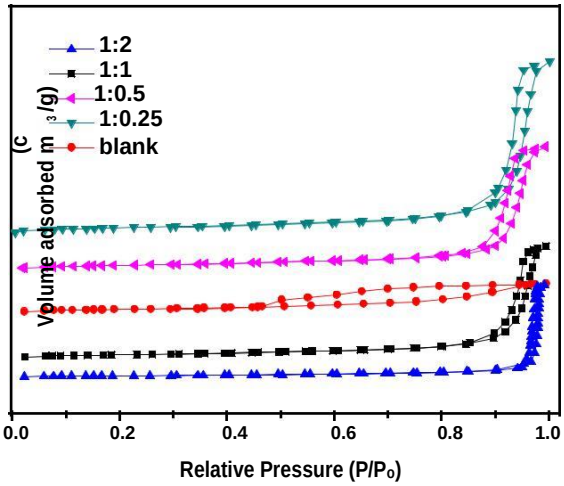

Figure 5.7: N_2 adsorbtion-desorbtion isotherm of MgO with different ratio of surfactant.

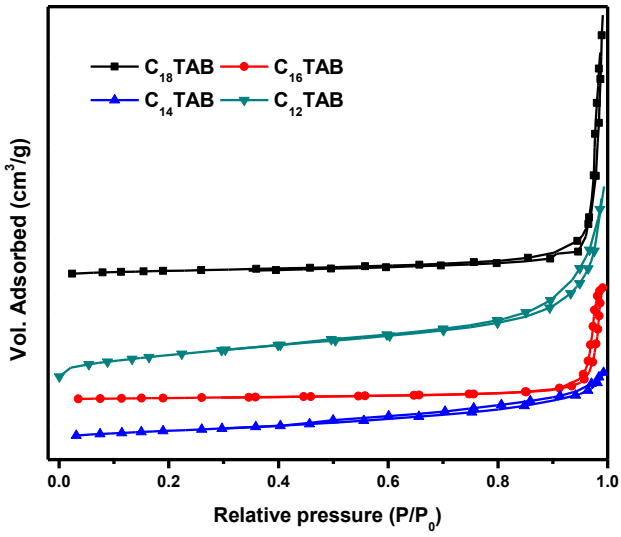

Figure 5.8: N_2 adsorbtion-desorbtion isotherm of MgO with different chain length of cationic surfactant.

CHAPTER 6 - APPLICATIONS

Adsorption study:

The variation of adsorption with pressure at a given constant temperature is generally expressed graphically. Each curve is known as adsorption isotherm for the particular temperature. The relationship between the magnitude of adsorption and pressure can be expressed mathematically by an empirical equation commonly known as **Freundlich adsorption isotherm**.

$$a = kp^n \quad (1)$$

$$\log q_e = \log K_f + (1/n) \log c_e \quad (2)$$

Where 'a' is the amount of the gas desorbed per unit mass of the adsorbent at pressure p, and k and n are constants depending upon the nature of the gas and the nature of the adsorbent. The value of n is less than 1 and therefore, a does not increase as rapidly as p, as is evident from the adsorption isotherms.

Langmuir isotherm:

In 1916, Langmuir proposed his theory of adsorption of a gas on the surface of a solid. He considered the surface of the solid to be made up of elementary sites each of which could adsorb one gas molecule. It is assumed that all adsorption sites are equivalent and the ability of the gas molecule to get bound to any one site is independent of whether or not the neighbouring sites are occupied. It is further assumed that a dynamic equilibrium exists between the adsorbed molecules and the free molecules. If A is the gas molecule and M is the surface site, then

$$A_{(g)} + M_{(surface)} \underset{K_d}{\overset{K_a}{\rightleftharpoons}} AM$$

$$\theta = \frac{K_p}{1 + K_p} \quad (2)$$

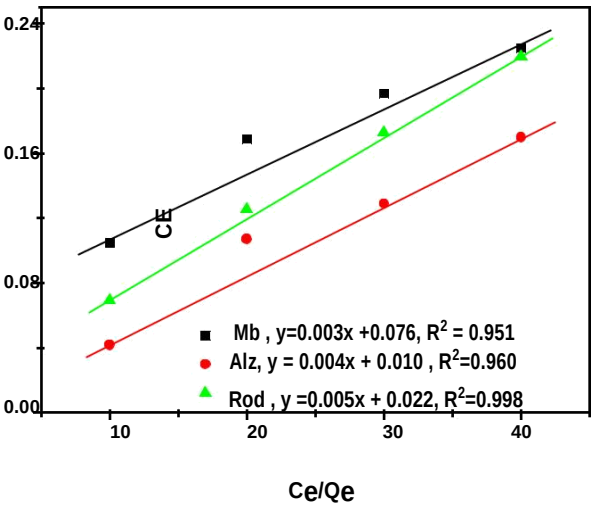

Figure 6.1: Langmuir isotherm for the adsorption of Mb, Alz, Rod onto mesoporous MgO

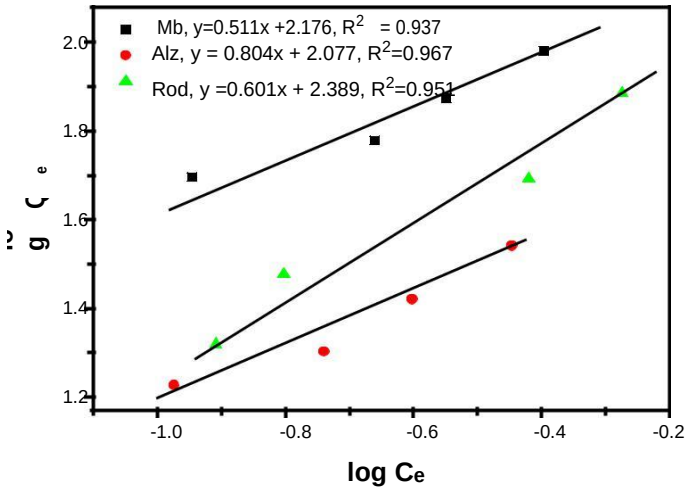

Figure 6.2: Freundlich isotherm for the adsorption of Mb, Alz, Rod onto mesoporous MgO.

Table 6.1: Langmuir and Freundlich constants and correlation coefficients for adsorption of different dyes on MgO.

DYE	Freundlich			Langmuir		
	K_f	N	R^2	Q_o	B	R^2
MB	380.18	1.95	0.937	333.33	0.7	0.951
Alz	244.90	1.66	0.951	250	0.4	0.960
Rod	119.39	1.24	0.967	200	0.118	0.998

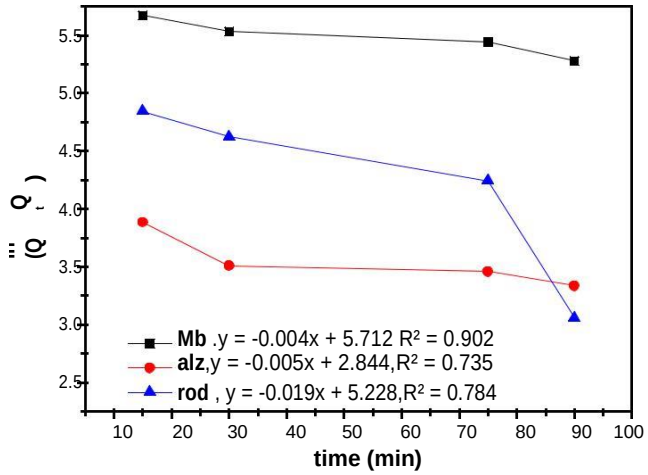

Figure 6.4: Linear fit curve of pseudo first order for Mb, Alz, Rod dyes onto mesoporous MgO.

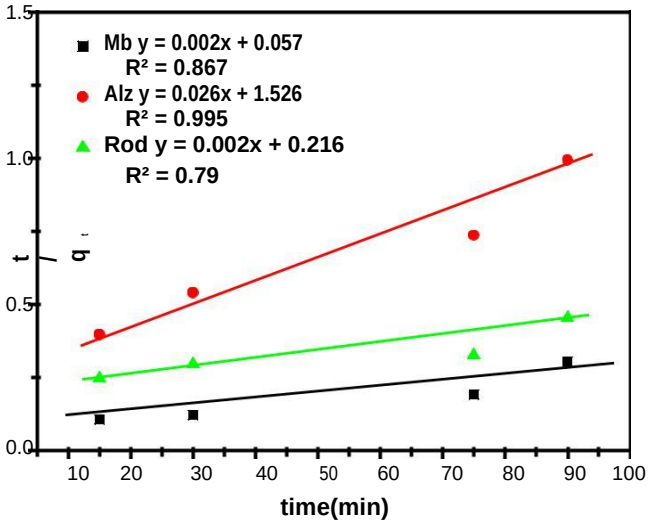

Figure 6.4: Linear fit curve of pseudo second order for the adsorption of Mb, Alz and Rod onto mesoporous MgO.

Effects of dye concentration:

Concentration of dyes affects the adsorption capacity of mesoporous MgO and it was determined under equilibrium environment with concentration of 100mg/L. The qe vs q_e/C_e , determines the adsorption capacity that it is increases with the increase in dyes concentration which results to increase in the mass gradient between solution and the adsorbent.

Dye adsorption on the magnesium-oxides was performed in a batch system at suitable temperature using favourable conditions. MgO (0.01g) was added into 100 ml of aqueous dye solution, (100-500 mgL^{-1}) under agitation, at a rate of 200 rpm.

In order to obtain the adsorption capacity (q), the uptake amount of dye and metal ions adsorbed per mass unit of MgO (mg/g) was calculated using the formula:

$$q_e = \frac{(C_o - C_e)}{m} \times V \qquad (3)$$

Where, C_o and C_e are the initial and the equilibrium concentrations (mg/L), while M and V are the weight of the adsorbent (g) and the volume of the solution (L).

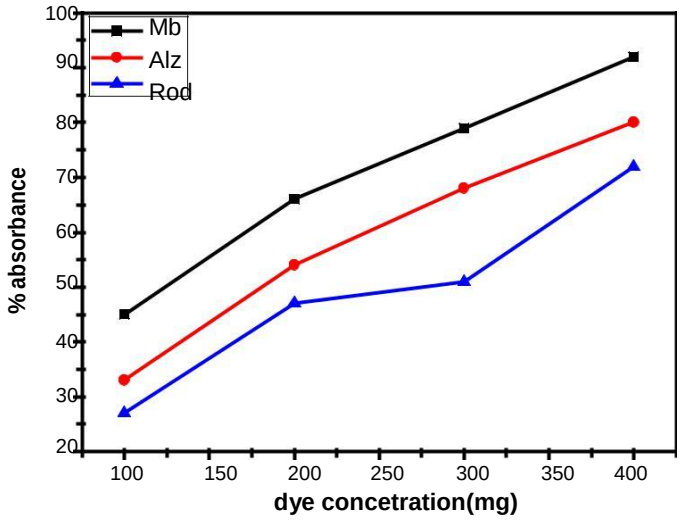

Figure 6.5: Effect of concentration of different dyes for adsorption on MgO

Effect of temperature on adsorption:

To determine the effect of temperature on dyes (i.e, Mb, Rod, Alz), MgO was treated at 313, 333 and 353 K. The observed decrease in both values of 1/T and ln(Qe/Ce) with high temperature indicates the exothermic nature of the adsorption process. The

values of ln(q_e/C_e) at different temperatures are treated according to Van't Hoff equation:

$$\ln\left(\frac{q_e}{C_e}\right) = \frac{-\Delta H}{RT} + \frac{\Delta S}{R} \quad (4)$$

Where R is the universal gas constant (8.314 J/ (mol K)) and T is the absolute temperature (in Kelvin). Plotting ln(q_e/c_e) against 1/T gives a straight line with slope and intercept equal to respectively.

The positive value ofΔH shows endothermic nature of adsorption process. The adsorption is favoured at higher temperature. Gibbs free energy of adsorption (ΔG) is calculated from the following relation:

$$\Delta G = \Delta H + T\,\Delta S \quad (5)$$

Negative value of ΔG, represents the spontaneous reaction of adsorption.

Table 6.2: Thermodynamic parameters at different temperatures for removal of Mb, Alz and Rod on MgO.

DYE	T(K)	ΔG (kJ mol^{-1})	ΔH (kJ mol^{-1})	ΔS (J $mol\ K^{-1}$)
Mb	303	-10.03	11.01	41.99
	313	-17.12		
	323	-21.3		
Rod	303	-8.2	9.72	35.99
	313	-11.81		
	323	-15.41		
Alz	303	-10.37	8.18	31.46
	313	-13.52		
	323	-16.6		

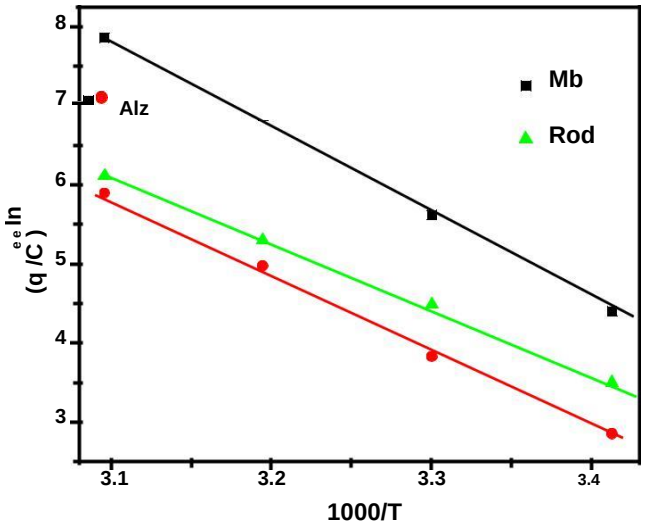

Figure 6.6 Van't hoff plot showing effect of temperature on different dyes on MgO.

Effect of contact time:

Contact time is the parameters which elaborated the efficiency of MgO on dyes. At 6 pH, the initial concentration of all the three dye (mb, alz, rod) of 500mg/L were taken. It was examined that with the increase in the time, there is increase adsorbance of dye concentration. Figure also indicated that methylene blue has the maximum adsorbance with time in comparison to alizarin and rhodamine. After 45 min the saturation point is observed in all the dye.

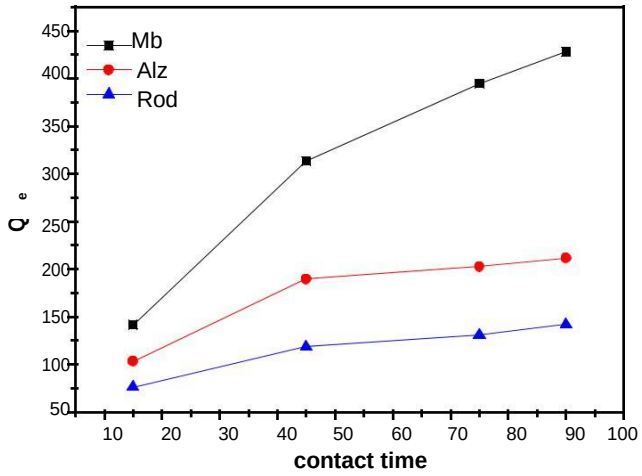

Figure 6.7: Effect of contact time on initial concentration of different dyes

Effect of pH:

pH is an significant parameter which affects both aqueous chemistry and surface binding sites of the adsorbents. The effect of initial pH values were demonstrated at different values ranging from 3 to 10 and adjusted by adding 0.1 M NaOH and 0.1 M HNO_3 solutions on the aqueous solution of methylene blue and kept stirring for 30min. Figure 6.6 shows the results of the effect of pH on different dyes removal efficiencies. All the dyes show maximum adsorption at pH 6 and the corresponding increase in percentage adsorsption for Mb, Alz and Rod using MgO increases from 76.4 to 96.8 %; 81.2 to 93.4% and 78.8 to 94.8%, respectively.

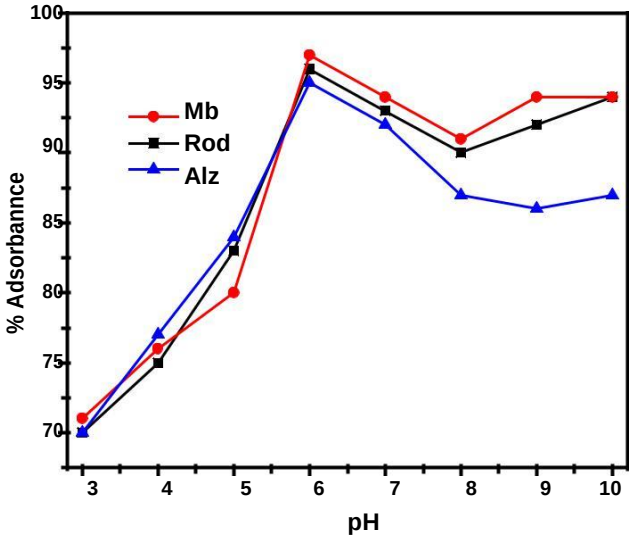

Figure 6.8: Effect of pH on different dyes using MgO

Antimicrobial activitiy:

The antimicrobial activities against *E.Coli* and *B.subtilis* of MgO were shown in Figure 6.8 the antimicrobial activity of MgO is proportional to the concentration of the nanorods are used. The IC_{50} values obtained after 24h of MgO incubation for *E.coli* and *B.subtilis* were 0.476±0.056 and 0.449±0.043 respectively.

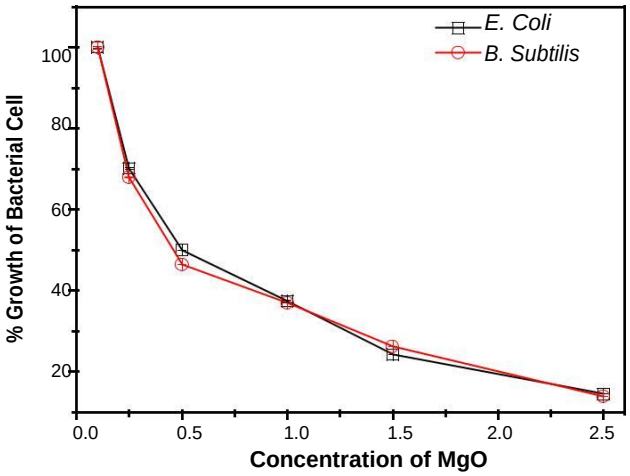

Figure 6.9: Concentration v/s %bacterial growth plot for antimicrobial activity using *E.coli* and *B.subtilis* on MgO

Conclusion

The recent study shows that the surface area of magnesium oxide can be increase with the use of mixture of surfactants i.e. cationic and anionic surfactants with a surfactant templating method. The morphology of mesoporous MgO nano-rods (20-60nm) was determined by FESEM, HRTEM and its crystalline size (30-45 nm) is determined by XRD. The mesoporous MgO shows high surface area (171.49 m^2 g^{-1}) with ratio 1:0.25 ($MgCl_2$: C_{16}tab + SDS). Different chain length of cationic surfactants also affects the surface area as well as the crystalline size of the nanostructures MgO. It is also shown that due to highest surface area of MgO it is also efficient in adsorption capacity and has (333.33, 250 and 200) mg g^{-1} for methylene blue, Alizarin and Rhodamine respectively. It is interesting to know that mesoporous MgO is also acts as a bactericide and its IC_{50} value for *E.Coli* and *B.Subtilis* were 0.476±0.056 and 0.449±0.043 respectively.

References

1. S. Balamurugan, L. Ashna and P. Parthiban, *J. Nanotechno* 2014, **2014**.
2. K. Kaviyarasu and P. A. Devarajan, *Chem. Inform* 2012, **43**, 248-254.
3. S. Suresh and D. Arivuoli, *Digest J Nanomater* 2011, **6**, 1597-1603.
4. F. Gu, S. F. Wang, M. K. Lü, W. G. Zou, G. J. Zhou, D. Xu, and D. R. Yuan, *J Cryst Growth* 2004, **260**, 507-510.
5. B. Nagappa and G. T. Chandrappa, *Microporous Mesoporous Mater.* 2007, **106**, 212-218.
6. S. M. Maliyekkal, Anshup, K. R. Antony, and T. Pradeep, *Sci. Total Environ.* 2010, **408**, 2273-2282.
7. K. V. Rao and C. S. Sunandana, *Synth React Inorg M* 2008, **38**, 173-180.
8. V. R. Orante-Barrón, L. C. Oliveira, J. B. Kelly, E. D. Milliken, G. Denis, L. G. Jacobsohn, J. Puckette, and E. G. Yukihara. *J.Lumin* 2011, **131**, 1058-1065.
9. I. E. Agranovski, A. Y. Ilyushechkin, I. S. Altman, T. E. Bostrom and M. Choi. *Physica C* 2006, **434**,115-120.
10. T. Mathews, R. Subasri and O. M. Sreedharan. *Solid State Ionics* 2002, **148**, 135-143.
11. N. Selvam, C. Sagaya, R. T. Kumar, L. J. Kennedy and J. J. Vijaya. *J Alloy Compd.* 2011, **509**, 9809-9815.
12. L. C. Oliveira, E. D. Milliken and E. G. Yukihara. *J.Lumin* 2013, **133** 211-216.
13. K. D. Bhatte, D. N. Sawant, K. M. Deshmukh and B. M. Bhanage.*Particuology* 2012, **10**, 384-387.

14. R. Kumar, A. Subramania, N. T. K. Sundaram, G. V. Kumar and I. Baskaran. J Membrane Sci 2007, **300**, 104-110.

15. F. Granados-Correa, J. Bonifacio-Martínez, V. H. Lara, P. Bosch and S. Bulbulian. *Appl Surf Sci* 2008, **254**, 4688-4694.

16. O. Diwald and E. Knözinger. *J Phys Chem B*. 2002, **106**, 3495-3502.

17. M. Anpo, Y. Yamada, Y. Kubokawa, S. Coluccia, A. Zecchina and M. Che. J Chem Sci.1988, **84**, 751-764.

18. D. M. Murphy, R. D. Farley, I. J. Purnell, C. C. Rowlands, A.l R. Yacob, M. C. Paganini and E. Giamello. *J Phys Chem B*.1999, **103**, 1944-1953.

19. R. Al-Gaashani, S. Radiman, Y. Al-Douri, N. Tabet and A. R. Daud. *J Alloy Compd*. 2012, **521**, 71-76.

20. K. Krishnamoorthy, G. Manivannan, S. J. Kim, K. Jeyasubramanian, and M. Premanathan. *J Nanopart Res*.2012, **14**, 1-10.

21. C. Henrist, J-P. Mathieu, C. Vogels, A. Rulmont, and R. Cloots. *J Cryst Growth*. 2003, **249**, 321-330.

22. F. Langenhorst. *J Miner*. 2001, **13**, 329-341.

23. Y. Ding, G. Zhang, H. Wu, B. Hai, L. Wang and Y. Qian. *Chem. Mater*. 2001, **13**, 435-440.

24. S. Utamapanya, K. J. Klabunde and John R. Schlup. *Chem. Mater*. 1991, **3**, 175-181.

25. A. Durin-France, L. Ferry, J-M. Lopez Cuesta, and A. Crespy. *Polymer International* 2000, **49**, 1101-1105.

26. G. Qing, Z. Junhua, C. Lin, X. Chang and H. Jiang. *Mater. Chem. Phys.* 2011, **130**, 387-391.

27. N. Kim, P. Hong, T. Lam and T. Huy. *J. Colloid Interf Sci*. 2013, **398**, 210-216.

28. K. R. Raghupathi, R. T. Koodali and Adhar C. Manna. *Langmuir*. 2011, **27**, 4020-4028.

29. K. H. Jung, K. Chu, S. T. Lee, H. K. Park, D. H. Kim, J. J. Bahm, E. C. Song. *J Cerebr Blood F Met.* 2008, **28**, 1795-1803.

30. J. Tony, and H.Yiping. *J Nanopart Res*. 2011, **13**, 6877-6885.

31. J. Sawai, *J Microbiol Meth*. 2003, **54**, 177-182.

32. T. Z. Xing, and B. Feng Lv. *Braz. J. Chem. Eng.* 2014, **31**, 591-601.

33. L. P., and L. Zhang. *Sep. Purif. Technol.* 2007, **58**, 32-39.

34. Ö. Y. M.Doğan and M. Alkan. *Microporous Mesoporous Mater*. 2006, **96**, 419-427.

35. N. K. Lazaridis, Z.K. George, A. V. Alexandros and N.B. Dimitrios. *Langmuir*. 2007, **23**, 7634-7643.

36. V. Bekiari and P. Lianos. *Chem. Mater*. 2006, **18**, 4142-4146.

37. S. P. Joaquim, S. Sousa, J. Rodrigues, H. Antunes, J.J. Porter, I. Gonçalves and S. F.Dias. *Sep. Purif. Technol.* 2004, **40**, 309-315.

38. A. Mittal, L. Krishnan and V. K. Gupta. *Sep. Purif. Technol.* 2005, **43**, 125-133.

39. H. Juncheng, Z. Song, C. Lifang, H. Yang, L. Jinlin and R. Richards. *J Chem Eng Data*.2010, **55**, 3742-3748.

40. L. C. Kung, K. S. Lin, C.-F. Wu, M. Lyu and C. Lo. *J Hazard Mater*. 2008, **150**, 494-503

41. M. Pagliaro, Nano-age: how nanotechnology changes our future, 2011, John Wiley & Sons.

42. Y. Jimmy, C. X. Anwu, L. Zhang, R. Song and W. Ling. *J Phys Chem B*, **108**, 64-70.

43. X. Yao, T.Luo, J. Yong, Y.X. Zhang, J.H. Liu and X.J.Huang. *J Phys Chem C*. 2011, **115**, 22242-22250

44. G. Cuiling, W. Zhang, L. Hongbian, L. Leiming and X. Zheng. *Crystal Growth and Design*. 2008, **8**, 3785-3790.

45. Z. Sheng and E. Ruckenstein. *Langmuir*. 2002, **18**, 734-743.